Evaluation of Gmax CPT correlations on an offshore site in the Netherlands

Reidy, S.; Klinkvort, R.T.; Anderson, E.; Jostad, H.P.; Gavin, K.

DOI
10.53243/ISFOG2025-203

Publication date
2025

Document Version
Final published version

Published in
Proceedings of ISFOG 2025

Proceedings of ISFOG 2025
5TH INTERNATIONAL SYMPOSIUM ON
FRONTIERS IN OFFSHORE GEOTECHNICS
Nantes, France | June 9-13 2025

ISBN 978-2-85782-758-0

Evaluation of G_{max} CPT correlations on an offshore site in the Netherlands

S. Reidy*
Norwegian Geotechnical Institute / Delft University of Technology, Oslo, Norway

R.T. Klinkvort, E. Anderson, H.P. Jostad
Norwegian Geotechnical Institute, Oslo, Norway

K. Gavin
Delft University of Technology, Delft, Netherlands

sinead.reidy@ngi.no (corresponding author)

ABSTRACT: This study reviews existing cone penetration test (CPT) correlations for the prediction of the small strain shear modulus (G_{max}). Its performance is investigated through application to an open-source offshore ground investigation dataset from the Netherlands. The research evaluates correlations involving various parameters such as cone tip and corrected cone tip resistance, net corrected cone resistance, sleeve friction, pore water pressure, and vertical effective stress. Results indicate that correlations are highly site-specific, often requiring recalibration to account for local conditions. Existing sand correlations provide more accurate predictions but tend to underpredict G_{max}, while clay-specific correlations tend to overpredict G_{max}, particularly in stiffer offshore clays. The study also highlights the need for further exploration of parameter normalisation to refine these correlations. This work represents an additional step in the understanding of CPT-based G_{max} predictions and their associated uncertainties, emphasizing the importance of developing robust, site-specific correlations for optimal offshore wind foundation design.

Keywords: Offshore Wind; CPT Correlations; G_{max}.

1 INTRODUCTION

The EU has set the target to reduce emissions by 45% by 2030 and to reach climate neutrality or net-zero emissions by 2050 (United Nations, 2024). This is a significant challenge that requires a global transition to more renewable forms of energy. Many countries have prioritised offshore wind as a key alternative energy source for decarbonising society (European Commission, 2024). The foundations of offshore wind turbines (OWT) account for approximately one-quarter of their overall cost (Oh et al., 2018). A better understanding of the soil parameters used in designing these foundations will, therefore, lead to a more cost-optimal solution.

The small strain shear modulus (G_{max}) is an important soil parameter used in the design of OWT foundations. G_{max} can be measured directly in resonance column laboratory tests but is also often estimated through the shear wave velocity (V_s) and an estimate of the density of the soil (ρ) using the following formula:

$$G_{max} = \rho \cdot V_s^2 \quad (1)$$

V_s can be measured in the laboratory using bender element tests (Dyvik & Madsus, 1985) or in situ using a Seismic Cone Penetration Test (SCPT). The results obtained from laboratory test results, especially from reconstituted samples, are subject to sample disturbance. Therefore, the use of SCPT to measure the in-situ shear wave velocity (V_s) is a preferred method to estimate G_{max} as it provides a better representation of in-situ conditions. Correlating CPT response to V_s measurements is attractive because it allows us to estimate V_s based on a standard CPT test. Several authors have calibrated correlations for example Moss & Schneider (2011), Hegazy & Mayne (1995), Mayne et al. (1993), Stuyts et al. (2022), L'Heureux & Long (2017), Taboada et al. (2013), Mayne (2007), Mayne & Rix (1995), Bouckovalas et al. (1989) and Jaime & Romo (1988). The correlations appear to be dependent on the empirical dataset they are calibrated to, and do not appear to be universal correlations that can match all datasets. Factors such as the depositional environment and mineralogy of the soils may play a role.

This paper aims to illustrate how these correlations perform on a dataset from an offshore wind site in the Netherlands and discuss the uncertainties seen in these types of correlations. Finally, we calibrate a new CPT correlation to the data set and use that to illustrate the

uncertainties that still exist in the correlation even when calibrated to site-specific data.

2 METHODOLOGY

The TNW (Ten Noorden Van De Waddeneilanden) database site is located approximately 56km off the north coast of the Netherlands and has a total surface area of 120km^2. The site will accommodate 700MW of offshore wind energy once complete.

The dataset consists of V_s measurements measured between two geophones spaced at 0.5m and SCPT data averaged over the same 0.5m. Together with V_s, the SCPT data consists of q_c (cone tip resistance), f_s (sleeve friction) and u_2 (pore water pressure) measurements.

The SCPT tip response is corrected for total stress (σ_{v0}) to give net corrected cone resistance: $q_{net} = q_t - \sigma_{v0}$ (where $q_t = q_c + u_2(1-a)$ and a = net area ratio of cone in use) to evaluate the true strength of the soil. CPT data is often normalised because of the stress dependency of soil strength and stiffness, as suggested by Robertson (1990):

$$Q_{tn} = \left(\frac{q_{net}}{p_{ref}}\right) / \left(\frac{\sigma'_{vo}}{p_{ref}}\right)^n \quad (2)$$

$$F_r = \left(\frac{f_s}{q_t - \sigma'_{vo}}\right) \cdot 100\% \quad (3)$$

Where n is a stress normalisation factor. When $n=1$, the normalised tip resistance (Q_{tn}) is called Q_t whereas when $n=0.5$, it is called q_{c1N}. p_{ref} is the atmospheric pressure (taken as 100kPa). σ'_{vo} = vertical effective stress = $\sigma_{vo} - u_0$ (u_0 = *hydrostatic pressure*). F_r is normalised friction resistance. Q_{tn} and F_r can be used to estimate the soil type that is penetrated by calculating the Soil Behaviour Index (I_c) (Robertson, 2016):

$$I_c = ((3.47 - \log Q_t)^2 + (\log F_r + 1.22)^2)^{0.5} \quad (4)$$

The magnitude of I_c indicates the soil type. E.g. I_c values smaller than 2.05 indicate sands, I_c larger than 2.95 indicates clays.

Similar to the SCPT response, the shear wave velocity can also be normalised to minimise the effect of effective stress (Kayen et al., 2013):

$$V_{s1} = V_s \left(\frac{p_a}{\sigma'_{vo}}\right)^{0.25} \quad (5)$$

Where V_{s1} and V_s (measured) are in m/s.

Violin plots and boxplots were combined to give an initial overview of the TNW database. These show the density distribution of the TNW data alongside the mean, median and interquartile ranges, with the dots showing outliers (Figure 1). The top left plot shows that most q_c values range from 0 – 30MPa. The top right plot shows that most I_c values range from 1.3 to 2.0, which indicates that the majority of tests were performed in sand. σ'_{vo} is concentrated from 0 – 200kPa. The tests were mainly performed with a seafloor CPT, therefore most tests were performed in the top 20 m. Very little data from 30 – 60m impacts the range of σ'_{vo} in the dataset. In general, the top soils along the monopile are of most interest i.e. the top 35m. V_s is concentrated from 200 – 400m/s.

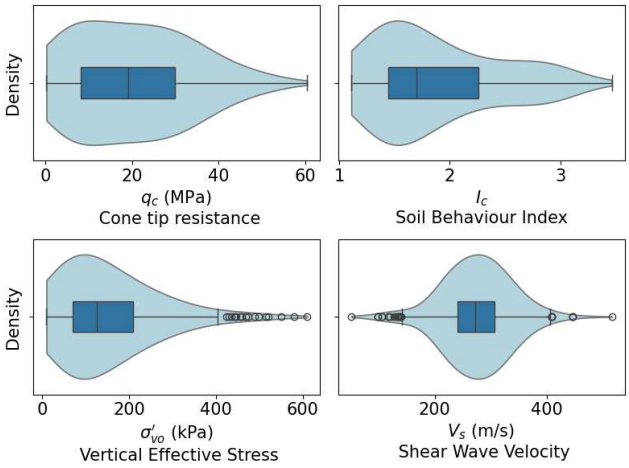

Figure 1 – Violin plot of TNW data

The following filtering criteria was applied to the data:

1) Data points < 5m below sea floor were excluded (as recommended in ISO 19901-8:2023). V_s measurement at shallow depths can be unreliable due to the location of the seismic source in relation to the SCPT (Seismic CPT) geophones.
2) Classification of sand, clay and transitional materials is based on soil behaviour index where I_c > 2.95 is a clay (diamond shape in scatter plots (Figure 3,Figure 5 & Figure 6)). Values < 2.95 are grouped into sand for simplicity in this paper (circle shape in scatter plots).
3) Sand correlations plot sand units only. Clay correlations plot clay units only. All soil correlations plot both sand and clay units as defined in Table 1 - Table 3.

The TNW data was collected to develop a geological ground model (GGM) for the offshore wind farm site. The ground model was developed based on an integrated interpretation of geology, geophysical, and geotechnical data. This led to a sequence of 20 units characterised by seismic architecture, basic

lithology, and chronostratigraphic origin. Details of this can be found in NGI (2022). The units are split into 6 main geological events:

- Holocene (GGM 02-03)
- Eemian and early Weichselian (GGM 11)
- Mid-to late Saalien (GGM 21-24)
- Holsteinian and early Saalien (GGM 31-33)
- Elsterian (GGM 51-54)
- Pre-Elsterian (GGM 61)

The I_c values were plotted in a stacked histogram to visualise the spread of sands (1.31-2.05), sand mixtures (2.05-2.60), silt mixtures (2.60-2.95) and clays (2.95-3.60) present in the dataset. Figure 2 indicates that the majority of the TNW dataset consists of sands followed by sand mixtures. The soil unit legend in Figure 2 is consistent with that for Figure 3 - Figure 6 in this paper.

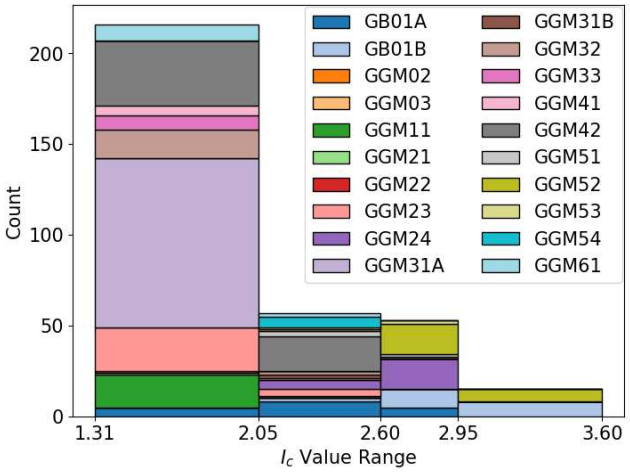

Figure 2 - I_c stacked histogram of TNW soil units

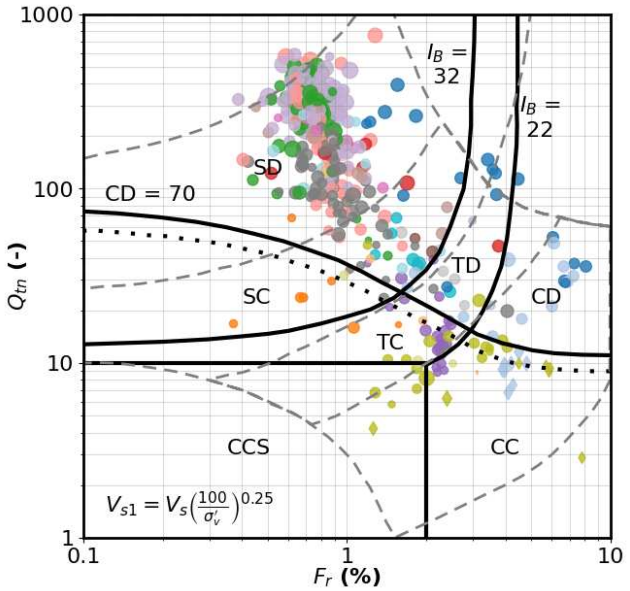

Figure 3 - Q_{tn} vs. F_r (Robertson 2016) plot with normalised shear wave velocity (V_{s1}) scatter markers

To further examine the dataset, F_r was plotted against Q_{tn}. Figure 3 defines the zones as per Robertson (2016). The marker size on the figures indicates the V_{s1} value. This allows us to see if there are any obvious correlations in the data. The majority of the data plots are in the sand-like dilative (SD) section of the plot, indicating that the TNW dataset is mainly made up of medium dense to dense sand units. No clear correlations are seen from this figure. A similar plot using G_{max}/q_t instead of V_{s1} did not show any clear correlation either.

To be able to compare the different calibration constants, all V_s correlations were converted to G_{max} format as part of this study, with density taken as 2Mg/m^3. L'Heureux & Long (2017) noted that correlations using f_s and those in log format are less accurate. Therefore, they were not included as part of this paper.

Table 1 shows the correlation using normalised tip resistance. The advantage of this correlation is that it is dimensionally correct. Most correlations are in the format shown in Table 2 with q_c as input. Table 3 shows some correlations for q_{net}. It is noted that q_{net} is only used for correlations in clay.

Table 1 – Correlations containing normalised q_{c1N}

	General Format	$G_{max} = K_G(q_{c1N})^{-m}q_t$		
	SAND	**K_G**	**m**	**q_t**
A	Moss & Schneider (2011)	330	0.75	q_t

Table 2 – Correlations containing q_c

	General Format	$G_{max} = C_1 q_c^{C_2} \sigma'^{C_3}_{vo}$		
	SAND	**C_1**	**C_2**	**C_3**
B	Hegazy & Mayne (1995)	347	0.38	0.36
C	Baldi et al. (1989)	610	0.26	0.54
D	Rix & Stokoe (1991)	1634	0.25	0.38
E	Stuyts et al. (2022)	2241	0.25	0.37
	CLAY	**C_1**	**C_2**	
F	Mayne & Rix (1995)	6	1.25	
G	Jaimo & Romo (1988)	0.02	2	
H	Bouckvolas et al. (1989)	2.8	1.4	
I	Mayne & Rix (1993)-All Clay sites	2.8	1.34	
	ALL SOILS			
M	Hegazy & Mayne (2006) - q_c	273	0.68	

Table 3 – Correlations containing q_{net}

	General Format	$G_{max} = C_1 q_{net}^{C_2} \sigma'^{C_3}_{vo}$		
	CLAY	**C_1**	**C_2**	**C_3**
K	L'Heureux & Long (2017)	139	0.44	0.71
L	Taboada (2013)–Eqn.13	415	0.53	0.27

The tables allow us to compare calibration constants directly, but the different format of the correlations makes a direct comparison difficult. To better understand the various correlations, we have plotted the different correlations assuming a constant vertical stress, pore pressure response equal to the hydrostatic pressure and with varying values of q_c and q_t. Figure 4 shows that sand correlations predict values in the range of 100-150MPa. Sand correlations have a smaller C_2 value than clay correlations. Four clay correlations are more exponential in shape with maximum q_c values of 5-12MPa. The typical q_t or q_c range for clays is 0-10MPa and 20-50MPa for sands. The sand and clay correlations distinctly separate around 5 MPa, reaffirming their differing behaviours. The zoomed in plot highlights the differing shape of the clay correlations in the 0-2MPa q_c or q_t range. G_{max} predicted is plotting approximately 400MPa for K, L (clay correlations) & M (correlation for all soils).

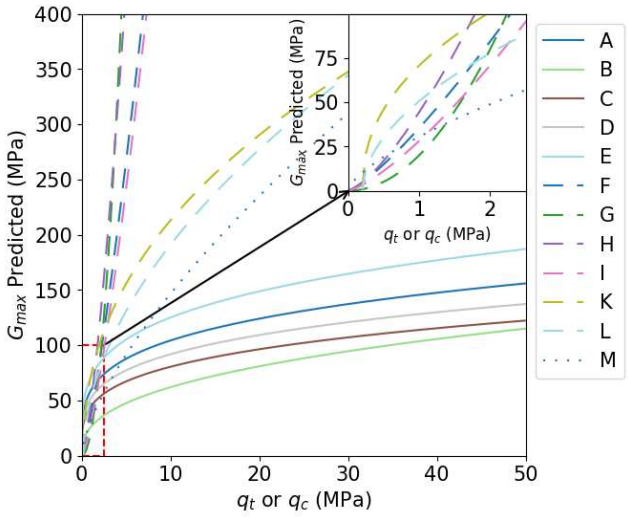

Figure 4 - G_{max} predicted vs. q_t or q_c (0-50MPa)

3 RESULTS

G_{max} predicted versus G_{max} measured was plotted for all correlations listed in Table 1-Table 3 to evaluate the performance of the CPT correlations found in literature (Figure 5). The red line is a 1:1 slope line. Should G_{max} predicted and G_{max} measured be equal, all datapoints would lie along this slope line. G_{max} is underpredicted in all sand correlations. Therefore, the G_{max} predicted points are mostly located below this 1:1 line. The opposite is the case for clays. The histogram in the top right corner of each graph depicts the statistical spread and frequency of the predictions about the 1:1 line. There is a normal distribution visible in the sand plots. This is not the case for the clay plots due to less clay data within the TNW dataset.

The study shows that in general, the correlations developed for sands correlate better. The most accurate sand correlations in literature are A and E. The TNW dataset was one of four used by Stuyts et al. (2022) in E and must be considered when viewing correlation results as it depicts a bias towards the TNW dataset. The range of q_t values in E is the same as that in the TNW dataset (0-60MPa).

For clay correlations, different parameters are used (q_{net}, q_c and σ'_{vo}) which result in differences in the results and scatter plotted. The L'Heureux & Long (2017) correlation was developed for soft clay sites so it may not be the most applicable for offshore as they are over-consolidated in this case. The Mayne & Rix (1993, 1995) correlations plot similar to L'Heureux & Long (2017) in terms of magnitude and overprediction of G_{max} values. These correlations were developed for clay sites onshore and therefore the stiffness and strength of the materials present in the TNW dataset are likely much larger than those in the datasets used for the development of previous correlations.

The Taboada et al. (2013) correlation (q_{net} = 0-8MPa) provides less spread of the G_{max} predicted data and therefore is a better fit. This better fit may be a co-incidence as the TNW site is over-consolidated, whereas the Gulf of Mexico clay is normally consolidated. It may, however, highlight that correlations developed for offshore sites are a better fit to the TNW data as they are more site specific.

The Jaime & Romo (1988) & Bouckovalas et al. (1989) correlations overpredict G_{max} from the TNW dataset. Three sites near Mexico City with highly plastic clays (q_c < 1MPa) and two Greek clay sites (q_c = 0-10MPa) were used to develop these correlations and therefore they are not the most applicable to the TNW dataset. The q_c values that are considered clays in the TNW dataset range from 0-6MPa and consist of very low strength clays (Naaldwijk) from the Holocene period, as well as medium to high strength clays (Peelo) from the Elsterian period (NGI, 2022).

The Hegazy & Mayne (2006) correlation is for all soils (q_c = 0.2-50MPa) and plots both sand and clay soil units. Most of the data lies above the 1:1 line, showing that this correlation overpredicts G_{max} values. The histogram in the top left corner is skewed left.

Results reiterate that the correlations in literature are all site specific. Figure 6 shows calibrations per soil unit. It clearly differentiates the clay, sand and transitional material. The slope of each soil unit line was extracted so that a corresponding K_G and m value could be found (similar to table 1 format). From reviewing both Figure 6 and the equations of the lines, the soil units GB01B and GGM52 (red arrows) can be linked together with visually identical slopes at the top of the plot (both clay layers). GGM24 and GGM53

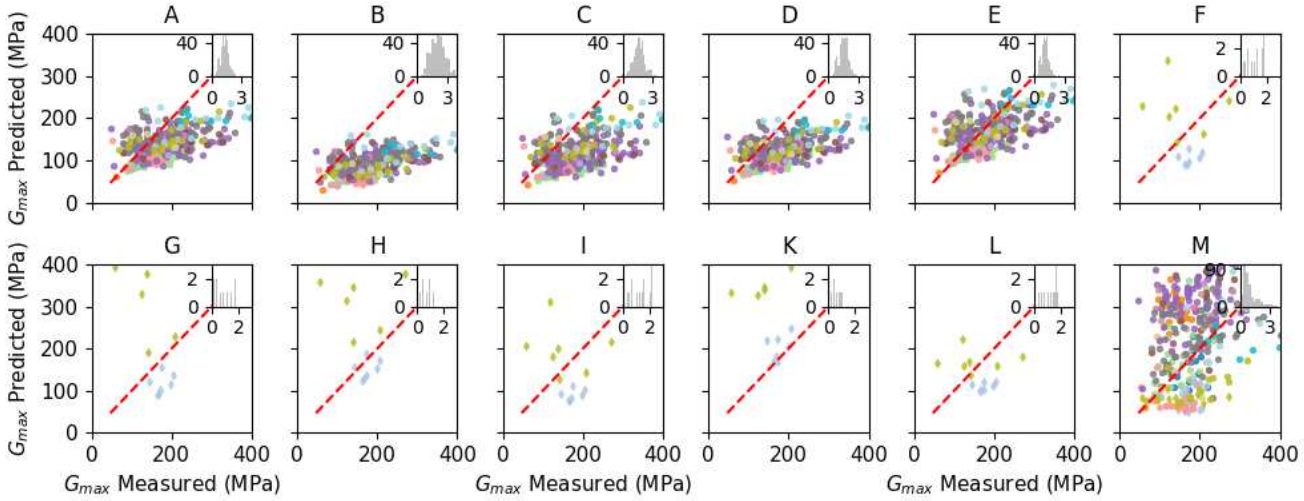

Figure 5 - G_{max} predicted vs. G_{max} measured for all correlations studied in literature

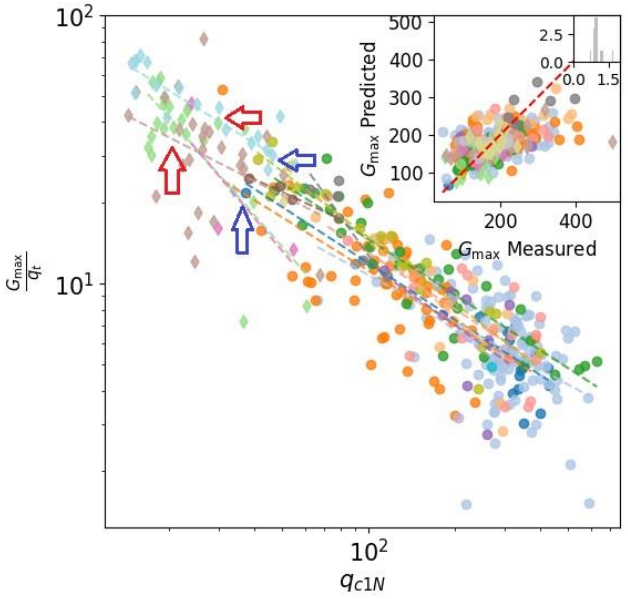

Figure 6- G_{max}/q_t vs. q_{c1N} for TNW dataset

(blue arrows) appear in a zone between clay and sand layers. They could potentially consist of transitional material. All sand layers appear to converge towards the same point and have very similar slopes.

The subplot of G_{max} predicted vs. G_{max} measured uses the slope and intercept from the main plot (Figure 6), along with q_t values to calculate G_{max} predicted for each soil unit. These values use the correlation made specifically using the TNW dataset and should lie perfectly along the 1:1 line. Here, as in the Figure 5 subplots, there is a large amount of scatter in the points plotted. The histogram in the corresponding subplot, follows a normal distribution with a narrow spread which is to be expected using the correlation developed for the TNW data. The correlation developed is the most accurate but still depicts a large amount of variation.

4 CONCLUSIONS

The work is a step towards a better understanding of CPT correlations for G_{max} and its associated uncertainties.

Key Findings:

1. Correlations are dependent on multiple parameters. Those studied in this research to date include:
   a. q_c (cone tip resistance),
   b. q_t (corrected cone tip resistance),
   c. q_{net} (net corrected cone tip resistance),
   d. f_s (sleeve friction)
   e. u_2 (pore water pressure)
   f. σ'_{vo} (in situ vertical effective stress)
2. Correlations developed to date are site specific and must be developed individually for each site. Factors such as aging, cementation, K_0 conditions may play an important role.
3. Normalisation of parameters in the current correlations should be further explored to get a better understanding of the impact each parameter has on the correlation in question.

In conclusion, the work to date reveals that for optimal foundation design, calibration of the correlation is needed and having a CPT correlation that works for Sand, Clay and Transitional soils is preferable.

AUTHOR CONTRIBUTION STATEMENT

S. Reidy: Figure curation, Methodology, Formal Analysis, Writing-Original draft. **R.T. Klinkvort, E.**

Anderson, H.P. Jostad & K. Gavin: Supervision, Writing-Reviewing & Editing.

ACKNOWLEDGEMENTS

The authors are grateful for the financial support provided by the FRONTIErS Doctoral Network – the European Union's Horizon Europe Programme under the Marie Skłodowska–Curie actions HORIZON-MSCA-2021-DN-01 call (Grant agreement ID: 101072360), and the UK Research and Innovation (Grant Ref: EP/X027910/1 and EP/X027821/1).

REFERENCES

Bouckovalas, G., Kalteziotis, N., Sabatakakis, N., & Zerogiannis, C. (1989). *Shear wave velocity in a very soft clay-Measurement and correlations*. https://www.issmge.org/publications/online-library

Commission, E. (2024). *Offshore renewable energy | European Commission*. https://energy.ec.europa.eu/topics/renewable-energy/offshore-renewable-energy_en

Dyvik, R., & Madsus, C. (1985). Lab Measurements of Gmax using Bender Elements. *Proceedings ASCE Annual Conventional: Advances in the Art of Testing Soils Under Cyclic Conditions,* 186–197.

Hegazy, Y. A., & Mayne, P. W. (1995). *Statistical correlations between Vs and CPT data for different soil types*. https://www.researchgate.net/publication/283361455

Hegazy, Y. A., & Mayne, P. W. (2006). A Global Statistical Correlation between Shear Wave Velocity and Cone Penetration Data. *Site and Geomaterial Characterisation (ASCE GSP 149), Proc GeoShaghai*, 243–248. https://doi.org/10.1061/40861(193)31

ISO 19901-8:2023. (2023). *ISO 19901-8:2023 Oil and Gas Industries including lower carbon energy Offshore structures. Part 8: Marine soil investigations*.

Jaime, A., & Romo, P. (1988). The Mexico Earthquake of September 19, 1985 - Correlations between Dynamic and Static Properties of Mexico City Clay. *Earthquake Spectra*.

Kayen, R., Moss, R. E. S., Thompson, E. M., Seed, R. B., Cetin, K. O., Kiureghian, A. Der, Tanaka, Y., & Tokimatsu, K. (2013). Shear-Wave Velocity–Based Probabilistic and Deterministic Assessment of Seismic Soil Liquefaction Potential. *Journal of Geotechnical and Geoenvironmental Engineering*, *139*(3), 407–419. https://doi.org/10.1061/(asce)gt.1943-5606.0000743

L'Heureux, J.-S., & Long, M. (2017). Relationship between Shear-Wave Velocity and Geotechnical Parameters for Norwegian Clays. *Journal of Geotechnical and Geoenvironmental Engineering*, *143*, 04017013. https://doi.org/10.1061/(ASCE)GT.1943-5606.0001645

Mayne, P. W. (2007). In-situ test calibrations for evaluating soil parameters. *Characterisation and Engineering Properties of Natural Soils*, *3–4*, 1601–1652. https://doi.org/10.1201/noe0415426916.ch2

Mayne, P. W., Nix, G. J., Mayne, R. :, & Rix, P. W. (1993). Gmax-qc Relationships for Clays. In *Geotechnical Testing Journal, GTJODJ* (Vol. 16, Issue 1). http://asmedigitalcollection.asme.org/geotechnicaltesting/article-pdf/16/1/54/7079022/10_1520_gtj10267j.pdf

Mayne, P. W., & Rix, G. J. (1995). Japanese Society of Soil Mechanics and Foundation Engineering - Correlations between shear wave velocity and cone tip resistance in natural clays. *Soils and Foundations* (Vol. 35, Issue 2).

Moss, R., & Schneider, J. (2011). Linking cyclic stress and cyclic strain based methods for assessment of cyclic liquefaction triggering in sands. *Géotechnique Letters*, *1*, 31–36. https://doi.org/10.1680/geolett.11.00021

Nations, U. (2024). *Net Zero Coalition | United Nations*. United Nations. https://www.un.org/en/climatechange/net-zero-coalition

NGI. (2022). *Ten noorden van de Waddeneilanden Wind Farm Zone - Geotechnical Interpretation Report. Rev.3*.

Oh, K. Y., Nam, W., Ryu, M. S., Kim, J. Y., & Epureanu, B. I. (2018). A review of foundations of offshore wind energy convertors: Current status and future perspectives. *Renewable and Sustainable Energy Reviews*, *88*, 16–36. https://doi.org/10.1016/J.RSER.2018.02.005

Robertson, P. K. (1990). Soil classification using the cone penetration test. *Canadian Geotechnical Journal*, *27*, 151–158.

Robertson, P. K. (2016). Cone penetration test (CPT)-based soil behaviour type (SBT) classification system — An update. *Canadian Geotechnical Journal*, *53*(12), 1910–1927. https://doi.org/10.1139/cgj-2016-0044

Stuyts, B., Sastre Jurado, C., Gomez Bautista, D., & Kheffache, A. (2022). Bayesian estimation of small-strain shear modulus from offshore CPT tests in the North Sea. *Cone Penetration Testing 2022 - Proceedings of the 5th International Symposium on Cone Penetration Testing, CPT 2022*, 722–727. https://doi.org/10.1201/9781003308829-106

Taboada, V. M., Inc, N., Cruz, D., Barrera, P., Mexicano del Petroleo, I., Espinosa, E., Carrasco, D., Mexicanos, P., Gan, K. C., & McClelland Marine Geosciences, F. (2013). Predictive Equations of Shear Wave Velocity for Bay of Campeche Clay. *Offshore Technology Conference*.